Cross sections for hard exclusive electroproduction of π^+ mesons on a hydrogen target

A. Airapetian,[15] N. Akopov,[25] Z. Akopov,[25] E.C. Aschenauer,[6] W. Augustyniak,[24] A. Avetissian,[25] E. Avetissian,[10] L. Barion,[9] S. Belostotski,[17] N. Bianchi,[10] H.P. Blok,[16,23] H. Böttcher,[6] C. Bonomo,[9] A. Borissov,[13] V. Bryzgalov,[18] J. Burns,[13] M. Capiluppi,[9] G.P. Capitani,[10] E. Cisbani,[20] G. Ciullo,[9] M. Contalbrigo,[9] P.F. Dalpiaz,[9] W. Deconinck,[15] R. De Leo,[2] M. Demey,[16] L. De Nardo,[5,21] E. De Sanctis,[10] M. Diefenthaler,[8] P. Di Nezza,[10] J. Dreschler,[16] M. Düren,[12] M. Ehrenfried,[12] G. Elbakian,[25] F. Ellinghaus,[4] R. Fabbri,[6] A. Fantoni,[10] S. Frullani,[20] D. Gabbert,[6] G. Gapienko,[18] V. Gapienko,[18] F. Garibaldi,[20] G. Gavrilov,[5,17,21] V. Gharibyan,[25] F. Giordano,[9] S. Gliske,[15] H. Guler,[6] C. Hadjidakis,[10] D. Hasch,[10] G. Hill,[13] A. Hillenbrand,[8] M. Hoek,[13] I. Hristova,[6] Y. Imazu,[22] A. Ivanilov,[18] H.E. Jackson,[1] S. Joosten,[11] R. Kaiser,[13] T. Keri,[12] E. Kinney,[4] A. Kisselev,[14,17] M. Kopytin,[6] V. Korotkov,[18] P. Kravchenko,[17] V.G. Krivokhijine,[7] L. Lagamba,[2] R. Lamb,[14] L. Lapikás,[16] I. Lehmann,[13] P. Lenisa,[9] L.A. Linden-Levy,[14] A. Lopez Ruiz,[11] W. Lorenzon,[15] S. Lu,[12] X. Lu,[22] D. Mahon,[13] N.C.R. Makins,[14] B. Marianski,[24] H. Marukyan,[25] C.A. Miller,[21] Y. Miyachi,[22] V. Muccifora,[10] M. Murray,[13] A. Mussgiller,[8] E. Nappi,[2] Y. Naryshkin,[17] A. Nass,[8] M. Negodaev,[6] W.-D. Nowak,[6] L.L. Pappalardo,[9] R. Perez-Benito,[12] N. Pickert,[8] M. Raithel,[8] P.E. Reimer,[1] A.R. Reolon,[10] C. Riedl,[10] K. Rith,[8] S.E. Rock,[5] G. Rosner,[13] A. Rostomyan,[5] L. Rubacek,[12] J. Rubin,[14] D. Ryckbosch,[11] Y. Salomatin,[18] A. Schäfer,[19] G. Schnell,[11] K.P. Schüler,[5] B. Seitz,[13] C. Shearer,[13] T.-A. Shibata,[22] V. Shutov,[7] M. Stancari,[9] M. Statera,[9] J.J.M. Steijger,[16] H. Stenzel,[12] J. Stewart,[6] F. Stinzing,[8] J. Streit,[12] S. Taroian,[25] E. Thomas*,[10] A. Trzcinski,[24] M. Tytgat,[11] A. Vandenbroucke,[11] P.B. van der Nat,[16] G. van der Steenhoven,[16] Y. van Haarlem,[11] C. van Hulse,[11] M. Varanda,[5] D. Veretennikov,[17] V. Vikhrov,[17] I. Vilardi,[2] C. Vogel,[8] S. Wang,[3] S. Yaschenko,[8] H. Ye,[3] Z. Ye,[5] S. Yen,[21] W. Yu,[12] D. Zeiler,[8] B. Zihlmann,[11] and P. Zupranski[24]

(The HERMES Collaboration)

[1] *Physics Division, Argonne National Laboratory, Argonne, Illinois 60439-4843, USA*
[2] *Istituto Nazionale di Fisica Nucleare, Sezione di Bari, 70124 Bari, Italy*
[3] *School of Physics, Peking University, Beijing 100871, China*
[4] *Nuclear Physics Laboratory, University of Colorado, Boulder, Colorado 80309-0390, USA*
[5] *DESY, 22603 Hamburg, Germany*
[6] *DESY, 15738 Zeuthen, Germany*
[7] *Joint Institute for Nuclear Research, 141980 Dubna, Russia*
[8] *Physikalisches Institut, Universität Erlangen-Nürnberg, 91058 Erlangen, Germany*
[9] *Istituto Nazionale di Fisica Nucleare, Sezione di Ferrara and Dipartimento di Fisica, Università di Ferrara, 44100 Ferrara, Italy*
[10] *Istituto Nazionale di Fisica Nucleare, Laboratori Nazionali di Frascati, 00044 Frascati, Italy*
[11] *Department of Subatomic and Radiation Physics, University of Gent, 9000 Gent, Belgium*
[12] *Physikalisches Institut, Universität Gießen, 35392 Gießen, Germany*
[13] *Department of Physics and Astronomy, University of Glasgow, Glasgow G12 8QQ, United Kingdom*
[14] *Department of Physics, University of Illinois, Urbana, Illinois 61801-3080, USA*
[15] *Randall Laboratory of Physics, University of Michigan, Ann Arbor, Michigan 48109-1040, USA*
[16] *National Institute for Subatomic Physics (Nikhef), 1009 DB Amsterdam, The Netherlands*
[17] *Petersburg Nuclear Physics Institute, St. Petersburg, Gatchina, 188350 Russia*
[18] *Institute for High Energy Physics, Protvino, Moscow region, 142281 Russia*
[19] *Institut für Theoretische Physik, Universität Regensburg, 93040 Regensburg, Germany*
[20] *Istituto Nazionale di Fisica Nucleare, Sezione Roma 1, Gruppo Sanità and Physics Laboratory, Istituto Superiore di Sanità, 00161 Roma, Italy*
[21] *TRIUMF, Vancouver, British Columbia V6T 2A3, Canada*
[22] *Department of Physics, Tokyo Institute of Technology, Tokyo 152, Japan*
[23] *Department of Physics and Astronomy, Vrije Universiteit, 1081 HV Amsterdam, The Netherlands*
[24] *Andrzej Soltan Institute for Nuclear Studies, 00-689 Warsaw, Poland*
[25] *Yerevan Physics Institute, 375036 Yerevan, Armenia*

(Dated: June 29, 2007)

The exclusive electroproduction of π^+ mesons was studied with the HERMES spectrometer at the DESY laboratory by scattering 27.6 GeV positron and electron beams off an internal hydrogen gas target. The virtual-photon cross sections were measured as a function of the Mandelstam variable t and the squared four momentum $-Q^2$ of the exchanged virtual photon. A model calculation based on Generalized Parton Distributions is in fair agreement with the data at low values of $|t|$ if power corrections are included. A model calculation based on the Regge formalism gives a good description of the magnitude and the t and Q^2 dependences of the cross section.

PACS numbers: 13.60.-r, 13.60.Le, 13.85.Lg, 14.20.Dh, 14.40.Aq

The interest in hard exclusive processes has grown since a Quantum Chromodynamics (QCD) factorization theorem was proven for the hard electroproduction of mesons by longitudinal photons [1]. It was shown that at leading order in the strong-coupling constant α_S and in the fine-structure constant α the amplitude for such reactions can be factorized into three parts (see left panel of Fig. 1): a hard lepton-scattering part, which can be calculated in Quantum Electrodynamics and in perturbative QCD (pQCD), and two soft parts that parametrize the structure of the target nucleon by Generalized Parton Distributions (GPDs) [2–4] and the structure of the produced meson by a distribution amplitude. The GPDs offer the possibility to reveal a three-dimensional representation of the structure of hadrons at the partonic level, correlating the longitudinal momentum fraction to transverse spatial coordinates [5–9]. For recent theoretical reviews, see Refs. [10–12].

The amplitude for exclusive electroproduction of mesons with specific quantum numbers is described by a particular combination of GPDs. At leading twist, exclusive vector-meson production is sensitive to only unpolarized GPDs (H and E), while pseudoscalar-meson production is sensitive to polarized GPDs ($\widetilde{H}$ and $\widetilde{E}$) without the need for a polarized target or beam. Moreover, for π^+ production, the pseudoscalar contribution involving $\widetilde{E}$ dominates at small momentum transfer to the target as it contains the $t-$channel pion-pole contribution. The complete amplitude of that contribution to π^+ production also contains the pion charge form factor [13, 14].

At moderate virtuality of the exchanged photon, next-to-leading-order (NLO) in α_S and higher-twist corrections to the pQCD leading-order amplitude can contribute. Two different types of higher-twist corrections, jointly denoted by the term "power corrections", have been estimated in the case of π^+ production [15]: one arising from the intrinsic transverse momentum of the partons, and the other resulting from the soft-overlap diagram. In contrast to the leading-order perturbative mechanism, the latter, shown on the right panel of Fig. 1, does not proceed through one-gluon exchange. Although significant NLO corrections have been calculated [16, 17], the higher-twist corrections dominate for the virtuality of the exchanged photon of the present data.

Alternatively, exclusive processes can be described at the hadronic level within the Regge formalism (e.g. [18]) where the interaction between the virtual photon and the nucleon is described in terms of Regge-trajectory exchanges in the t-channel. This approach can describe photoproduction [19] and electroproduction [20] of pseudoscalar mesons above the resonance region. In the latter case, meson production by both transverse and longitudinal photons contribute and can be calculated within the Regge formalism.

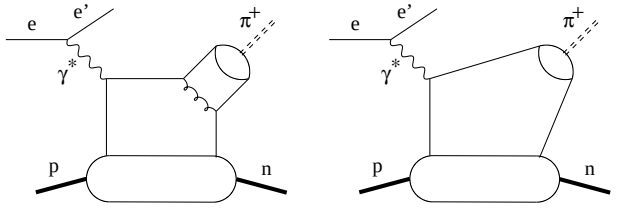

FIG. 1: Leading-order (left panel) and soft-overlap (right panel) diagram for the exclusive π^+ electroproduction amplitude.

This letter reports a measurement of the virtual-photon cross section for the hard exclusive reaction $ep \to en\pi^+$ on a hydrogen target. The relevant kinematic variables of the process are the squared four-momentum $-Q^2$ of the exchanged virtual photon, either the Bjorken variable $x_B = Q^2/2M_p\nu$ (where M_p is the proton mass and ν is the energy of the virtual photon in the target rest frame) or the squared invariant mass of the photon-nucleon system W^2, the Mandelstam variable t, and the azimuthal angle ϕ of the pion around the virtual photon momentum relative to the lepton scattering plane. Instead of t, the quantity $t' = t - t_0$ was used in the analysis, where $-t_0$ represents the minimum value of $-t$ for a given value of Q^2 and x_B.

The virtual-photon cross section has been previously measured above the resonance region (for $W^2 > 4$ GeV^2) at Cea [21], Cornell [22], Desy [23], and more recently at JLab [24, 25]. The present measurement extends the kinematic region to higher values of W and higher values of $-t'$.

The data were collected with the Hermes spectrometer [26] during the period 1996-2005. The 27.6 GeV Hera electron or positron beam at Desy scattered off polarized and unpolarized proton targets. Events were selected in which only one lepton and one positively charged hadron were detected and in which no additional cluster was recorded by the electromagnetic calorimeter. The Hermes geometrical acceptance of ± 170 mrad horizontally and $\pm(40 - 140)$ mrad vertically results in detected scattering angles ranging from 40 to 220 mrad. Leptons were distinguished from hadrons with an average efficiency of 98% and a hadron contamination less than 1% by using an electromagnetic calorimeter, a transition-radiation detector, a preshower scintillation counter, and a threshold gas Čerenkov counter. In 1998 the thresh-

*Present address: CERN, Geneva, Switzerland

old gas Čerenkov counter was replaced by a Ring Imaging Čerenkov detector [27]. The threshold gas Čerenkov counter (Ring Imaging Čerenkov detector) provided pion identification in the momentum range 4.9 GeV $< p <$ 15 GeV (1 GeV $< p <$ 15 GeV). For the exclusive data sample, the pion momentum was required to be 7 GeV $< p <$ 15 GeV. For this momentum range, the pion identification efficiency is on average 97% (99%) and the contamination from other hadrons less than 3% (2%) for the threshold gas Čerenkov counter (Ring Imaging Čerenkov detector).

The kinematic requirement $Q^2 > 1$ GeV^2 was imposed on the scattered lepton in order to select the hard scattering regime. The value of W^2 was required to be higher than 10 GeV^2 to avoid the low-acceptance region for the hadron defined by the spectrometer upper angular limit of 220 mrad. The resulting kinematic range is 1 GeV^2 $< Q^2 <$ 11 GeV^2 and $0.02 < x_B < 0.55$. The mean W^2 value of the data is 16 GeV^2.

As the recoiling neutron was not detected, exclusive meson production was selected by requiring that the squared missing mass M_X^2 of the reaction $ep \to e\pi^+X$ corresponds to the squared neutron mass. Due to the limited experimental resolution, the exclusive π^+ channel cannot be separated from the neighboring channels (defined as background channels) with final states such as $\pi^+ + (N\pi)$ and $\pi^+ + (N\pi\pi)$, as their M_X^2 values can be smeared into the region corresponding to exclusive π^+ channel. In order to subtract the background channels, which cannot be fully described by existing Monte Carlo simulations, a two-step procedure was developed. In the first step, the yield difference between π^+ and π^- was used. In this yield difference, exclusive π^+ events remain as the exclusive production of π^- on a hydrogen target with a recoiling nucleon in the final state is forbidden by charge conservation. Background events arising from the production of neutral vector mesons cancel as they contribute equally to π^+ and π^- production. In the second step, the PYTHIA Monte Carlo generator [28] was used in conjunction with a special set of JETSET [29] fragmentation parameters tuned to provide an accurate description of deep inelastic hadron production in the HERMES kinematic domain. The difference $\mathsf{N}_{\pi^+} - \mathsf{N}_{\pi^-}$, where N represents the yield normalized by the integrated luminosity $\mathcal{L}$, is well described by PYTHIA if pion momenta larger than 7 GeV are required. The latter constraint removes mainly background events for which $Q^2 < 3$ GeV^2. The upper panel of Fig. 2 shows the M_X^2 dependence of the normalized-yield difference $\mathsf{N}_{\pi^+} - \mathsf{N}_{\pi^-}$ for the data and for the PYTHIA Monte Carlo simulation. The Monte Carlo sample describes the data for values of the squared missing mass higher than 2 GeV^2, i.e., outside the region corresponding to exclusive π^+ production. Finally, the exclusive π^+ yield was obtained by subtracting the normalized-yield difference of the PYTHIA Monte Carlo from that of the data:

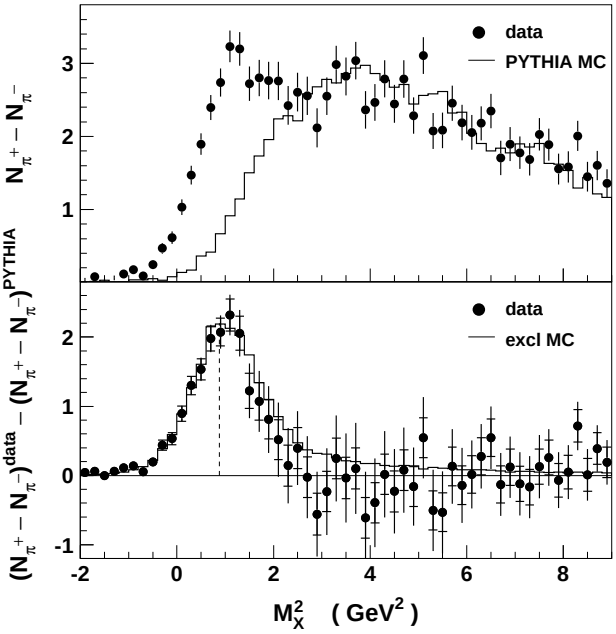

FIG. 2: Upper panel: squared missing-mass dependence of the normalized-yield difference $\mathsf{N}_{\pi^+} - \mathsf{N}_{\pi^-}$ for data (filled points) and PYTHIA Monte Carlo (histogram). The error bars represent the statistical uncertainty. Lower panel: squared missing-mass dependence of the normalized-yield after background subtraction procedure. The data (filled points) are compared to a Monte Carlo sample for exclusive π^+ production (histogram) normalized to the data. The inner error bars represent the statistical uncertainties and the outer error bars represent the quadratic sum of statistical and systematic uncertainties. The latter originate from the background subtraction procedure. The dashed vertical line indicates the squared neutron mass.

$\mathsf{N}^{\mathsf{excl}}_{\pi^+} = (\mathsf{N}_{\pi^+} - \mathsf{N}_{\pi^-})^{\mathsf{data}} - (\mathsf{N}_{\pi^+} - \mathsf{N}_{\pi^-})^{\mathsf{PYTHIA}}$. The lower panel of Fig. 2 shows the peak corresponding to exclusive π^+ production resulting from this double difference. The peak is centered at the squared neutron mass and its width of 0.67 GeV^2 is consistent with that of a Monte Carlo sample for exclusive π^+ production normalized to the data. The Monte Carlo, denoted as exclusive Monte Carlo, is based on a GPD model [15] and will be described below. As PYTHIA does not simulate nucleon resonance production, the agreement of the exclusive Monte Carlo sample with the data for the double difference is an indication that there is very little contribution from resonant channels ($\pi^+ + \Delta^0$ for π^+ and $\pi^- + \Delta^{++}$ for π^-) to the normalized-yield difference $\mathsf{N}_{\pi^+} - \mathsf{N}_{\pi^-}$. In order to estimate the systematic uncertainty of the background subtraction, the PYTHIA Monte Carlo normalized-yield difference $(\mathsf{N}_{\pi^+} - \mathsf{N}_{\pi^-})^{\mathsf{PYTHIA}}$ was changed by the discrepancy between that normalized-yield and the data in the region $3 < M_X^2 < 7$ GeV^2. The discrepancy amounts to between 20% and 50%, depending on the specific kinematic bin in Q^2, x_B, or t'. The largest discrepancies cor-

respond to the least populated bins ($Q^2 > 4$ GeV^2 and $-t' > 0.3$ GeV^2). An upper limit on M_X^2 of 1.2 GeV^2 was chosen in order to optimize the combined statistical and systematic uncertainties for the number of exclusive events. The resulting relative systematic uncertainty for the number of exclusive events ranges from 5% to 20%. Within the M_X^2 limit, the fraction of background events in the normalized-yield difference $\mathsf{N}_{\pi^+} - \mathsf{N}_{\pi^-}$ estimated with PYTHIA amounts to 20%. The number of π^+ events after background subtraction is 4510.

As the recoiling neutron was not detected, t' was determined from the measurement of the four-momenta of the scattered lepton and the produced pion. In order to improve the resolution for exclusive events, t' was calculated by setting $M_X = M_n$. This offered the possibility to discard the lepton energy, the quantity subject to the largest uncertainty for the present data sample. This procedure results in a factor of two improvement in the t' resolution. The same calculation was applied to the PYTHIA Monte Carlo events that were used to subtract the background.

The differential cross section for exclusive π^+ production by virtual photons can be written as

$$\frac{d\sigma^{\gamma^* p\to n\pi^+}(x_B,Q^2,t',\phi)}{dt'd\phi} = \frac{1}{\Gamma_V(x_B,Q^2)}\frac{d\sigma^{ep\to en\pi^+}(x_B,Q^2,t',\phi)}{dx_B dQ^2 dt' d\phi}, \quad (1)$$

where Γ_V is the virtual-photon flux factor. Within the Hand convention [30], this flux factor is

$$\Gamma_V(x_B,Q^2) = \frac{\alpha}{8\pi}\frac{1}{M_p^2 E^2}\frac{Q^2}{x_B^3}\frac{1-x_B}{1-\epsilon}, \quad (2)$$

where E is the beam energy and ϵ is the virtual-photon polarization parameter. The t' dependence of the photon-nucleon differential cross section integrated over ϕ were extracted from the data as follows:

$$\frac{d\sigma^{\gamma^* p\to n\pi^+}(x_B,Q^2,t')}{dt'} = \frac{1}{\Gamma_V}.\frac{N_{\pi^+}^{excl}}{\mathcal{L}\ \Delta x_B\ \Delta Q^2\ \Delta t'\ \kappa\ \eta}, \quad (3)$$

where $N_{\pi^+}^{excl}$ is the number of π^+ events after background subtraction, κ is the probability to detect the scattered lepton and the produced π^+ within the HERMES spectrometer acceptance, and η is the radiative correction factor. These quantities were determined for each kinematic bin. The symbols Δx_B, ΔQ^2, and $\Delta t'$ denote the bin size, which was chosen according to the statistical precision, instrumental resolution, and kinematic smearing affecting each individual bin. The t' dependence of the differential cross section $\frac{d\sigma(x_B,Q^2,t')}{dt'}$ was determined for four Q^2 bins and the Q^2 dependence of the cross section integrated over t', $\sigma(x_B,Q^2)$, for three x_B bins.

The detection probability κ was determined using an exclusive π^+ Monte Carlo simulation based on a GPD model [15] and a GEANT simulation [31] of the detector. The variable κ is the ratio between the number of simulated events reconstructed in the HERMES spectrometer and the number of generated events. These numbers were evaluated at the reconstructed and generated kinematics respectively and were integrated over the bin size and over ϕ (and t' for the determination of $\sigma(x_B,Q^2)$). The variable κ represents the combined effect of the spectrometer acceptance, the analysis constraints (such as the M_X^2 constraint) and the detector efficiencies. For the GPD model [15], the power corrections were included and the factorized ansatz was used for the t' dependence. However, the t' and ϕ dependences were modified in order to describe the data. Radiative events were included in the Monte Carlo simulation according to the code RADGEN [32] adapted to exclusive meson production [33] using the GPD model [15]. Fig. 3 shows the good agreement between the kinematic distributions of the data and of the exclusive Monte Carlo sample (which is normalized to the data by a constant factor) with the exception of yields at high values of $-t'$.

The calculated spectrometer acceptance ranges from 0.1 to 0.7 depending on the kinematic bin, while the efficiency of the detectors and analysis constraints together amounts to about 0.4–0.5. The combination of both leads to κ values ranging from 0.04 to 0.28. The model dependence of the determination of κ was estimated by using the GPD parametrization [15] with different t' and ϕ dependences and by using a different GPD parametrization [34] for the Q^2 and x_B dependences. This model dependence amounts to a relative systematic uncertainty on κ of less than 15%.

Events can be smeared from one bin to another by multiple scattering and bremsstrahlung. This effect was included in the determination of the detection probability κ. With the selected bin sizes, the fraction of events that migrate out of (into) a certain kinematic bin is on average 12% (15%) and is always below 25% (35%) according to the exclusive Monte Carlo simulation.

The Born cross section was extracted using the radiative correction factor η, which was determined from the ratio of Monte Carlo samples with and without radiative effects. The value of η was found to be 0.77 with little variation (less than 3%) as a function of Q^2, x_B or t' with the constraints applied to the data to select exclusive π^+ production.

The mean values for x_B, Q^2, and t' for each kinematic bin were estimated from distributions generated at Born level by the exclusive Monte Carlo simulation. The flux factor in Eq. 3 was determined for these mean values of Q^2 and x_B. The resulting cross sections were corrected for bin-averaging effects to take into account the nonlinear dependence of the cross section within each bin (in Eq. 3, a linear dependence inside a bin is implicitly assumed). These corrections were obtained from the exclusive Monte Carlo simulation by taking the ratio between

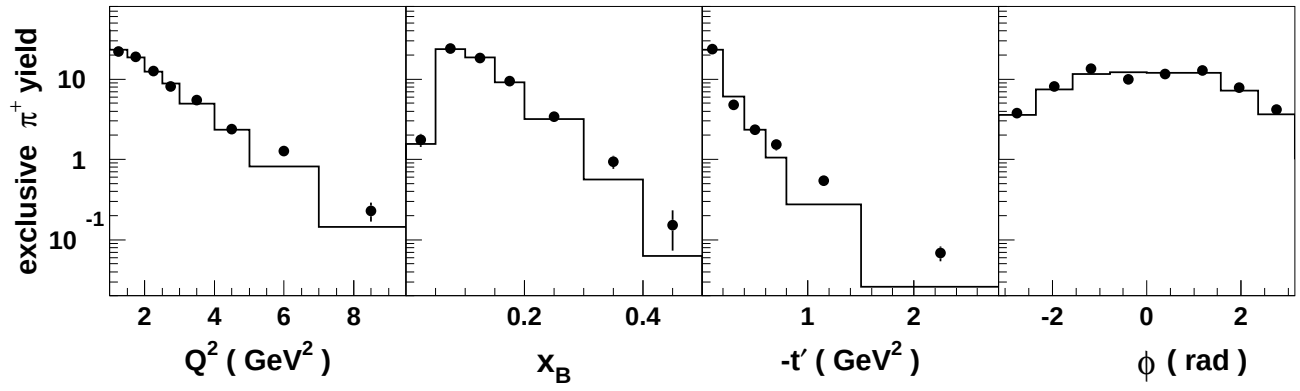

FIG. 3: Distributions of exclusive π^+ events within the HERMES acceptance as a function of Q^2, x_B, $-t'$ and ϕ for data (filled points) compared with an exclusive Monte Carlo simulation (histogram) based on a GPD parametrization [15] which was tuned to the data (see text). The data sample is arbitrarily normalized; the Monte Carlo sample is normalized to the data using a constant factor. The error bars represent the statistical and systematic uncertainties of the background subtraction added in quadrature.

the cross section evaluated at fixed kinematic values and the cross section integrated over the kinematic bins following Eq. 3. The error arising from the evaluation of the flux factor at the mean values is then also corrected. The bin-averaging correction factor amounts on average to 1.08 and does not exceed 1.2 except for the highest-Q^2 bin, where it reaches 2.2 at some t' values.

The integrated luminosity $\mathcal{L}$ was determined by comparing the number of inclusive deep-inelastic scattering events in the data sample to the yield generated by a Monte Carlo sample for inclusive scattering based on world data [35, 36]. The HERMES luminosity detector provided another measurement of $\mathcal{L}$, which was used to estimate the systematic uncertainty. The integrated luminosity $\mathcal{L}$ amounts to 0.4 fb^{-1} with a 5% systematic uncertainty.

The total systematic uncertainty of the cross section is dominated by the uncertainty of the background subtraction and of the detection probability. The latter takes into account the uncertainties due to the model dependence of its determination and the different detector resolutions in the different data taking periods.

The measured differential cross section integrated over the angle ϕ can be written as $\frac{d\sigma}{dt} = \frac{d\sigma_T}{dt} + \epsilon\frac{d\sigma_L}{dt}$ where σ_T and σ_L are, respectively, the contributions of transversely and longitudinally polarized virtual photons. At HERMES the separation of the transverse and longitudinal components of the cross section is not feasible. However, as the transverse contribution is predicted to be suppressed by $1/Q^2$ with respect to the longitudinal contribution [1], the data at larger Q^2 are expected to be dominated by the longitudinal part. Moreover, with the presence of the pion pole at low $-t'$, the longitudinal part of the cross section is expected to dominate in this region. In Fig. 4 and 5, described below, the data are compared to calculations for the longitudinal part of the cross section computed using a GPD model [15] and to calculations for the total cross section computed using a Regge model [37]. The cross sections are calculated for the mean values of x_B, Q^2, and t' of the experimental data in each bin.

Fig. 4 shows the t' dependence of the differential cross section for four Q^2 bins. As Q^2 is closely related to x_B (due to the HERMES acceptance as well as the upper limit on the pion momentum) low values of Q^2 correspond to low values of x_B. The dashed-dotted lines in Fig. 4 show the leading-order calculations of the longitudinal part computed using the GPD model [15]. The GPD $\widetilde{E}$ is considered to be dominated by the $t-$channel pion-pole and the pseudoscalar contribution to the cross section is parametrized in terms of the pion electromagnetic form factor F_π. A Regge-inspired t' dependence is used for $\widetilde{E}$. The GPD $\widetilde{H}$ is neglected here as $\widetilde{E}$ is expected to dominate the cross section at low $-t'$. The solid lines include the power corrections due to the intrinsic transverse momentum of the partons and due to the soft-overlap contribution, the latter being dominant. While the leading-order calculation strongly underestimates the data, the calculations including power corrections agree with the data for $-t' < 0.3$ GeV^2 for the four Q^2 bins. As the GPD model requires $-t'$ to be much smaller than Q^2, the calculations are not expected to describe the full t' range. Furthermore, at larger $-t'$, the data may receive a significant contribution from the transverse part of the cross section, which is not described by the GPD model. Fig. 5 shows the Q^2 dependence of the cross section integrated over t' for three x_B bins. The Q^2 dependence of the data is in general well described by the calculations from the GPD model [15] with the inclusion of the power corrections, although the magnitude of the cross section is underestimated. The data support the order of magnitude of the power corrections for the calculations by the

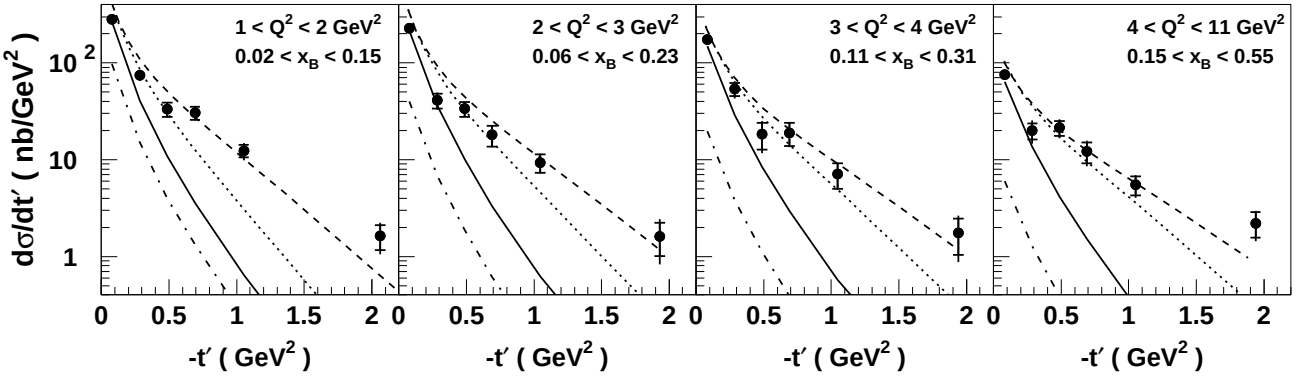

FIG. 4: Differential cross section for exclusive π^+ production by virtual photons as a function of $-t'$ for four Q^2 bins. The inner error bars represent the statistical uncertainties and the outer error bars represent the quadratic sum of statistical and systematic uncertainties. The curves represent calculations based on a GPD model [15] for $\frac{d\sigma_L}{dt'}$ using a Regge-type ansatz for the t' dependence (dashed-dotted lines: leading-order calculations, solid lines: with power corrections) and a Regge model [37] for $\frac{d\sigma}{dt}$ (dashed lines) and $\frac{d\sigma_L}{dt}$ (dotted lines).

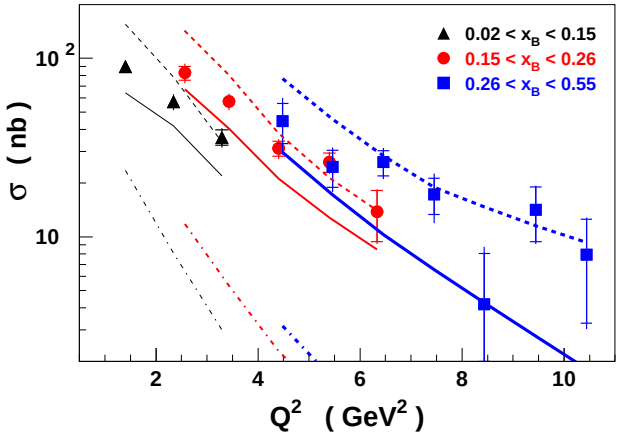

FIG. 5: Cross section for exclusive π^+ production by virtual photons as a function of Q^2 for three x_B bins and integrated over t'. The inner error bars represent the statistical uncertainties and the outer error bars represent the quadratic sum of statistical and systematic uncertainties. The curves represent calculations based on a GPD model [15] for σ_L using a Regge-type ansatz for the t' dependence (dashed-dotted lines: leading-order calculations, solid lines: with power corrections) and a Regge model [37] for σ (dashed lines). The thin, medium and thick lines correspond to the low, medium and high x_B values, respectively.

GPD model [15] at low $-t'$, a region where the longitudinal part of the cross section is expected to dominate, and for the available Q^2 range.

Both the transverse and longitudinal parts of the cross section were computed using a Regge model [37], where pion production is described by the exchange of π and ρ Regge trajectories. In this formalism, the meson-nucleon coupling constants are fixed by pion photoproduction data. In the original version [20], the $\pi\pi\gamma$ form factor is fixed by pion form factor measurements, while the $\pi\rho\gamma$ transition form factor is unconstrained. In the version used here [37], both form factors are taken to be both Q^2- and t'-dependent. The dashed (dotted) lines in Fig. 4 show the total (longitudinal) cross section computed using the Regge model. In this model the transverse part of the cross section is estimated to represent from 6% to 8% of the total cross section at $-t' = 0.07$ GeV^2 and from 15% to 25% of the total cross section integrated over t', confirming the expected suppression of the transverse to the longitudinal part of the cross section. However data from JLab [25] at lower center of mass energy ($W^2 = 4.9$ GeV^2) show that the transverse part of the cross section is underestimated by the Regge model by a factor of three to four. It is not clear if this also holds at the higher W^2 and $-t'$ values of the Hermes data. Compared to the calculations for the longitudinal cross section from the Regge model (dotted lines), the t' dependence of the GPD model [15] (solid lines) in Fig. 4 appears too steep. The total cross section computed by the Regge model describes well the t' dependence of the differential cross section (dashed line on Fig. 4) and the Q^2 dependence of the cross section integrated over t' (dashed lines on Fig. 5). The model calculations give also a good description of the magnitude of the data except at low $-t'$ for $Q^2 < 3$ GeV^2, where the calculations overestimate the data up to 70%.

In conclusion, the cross section was measured for exclusive electroproduction of π^+ mesons from a hydrogen target as a function of $-t'$ for four Q^2 bins and as a function of Q^2 for three x_B bins. A model calculation for the longitudinal part of the virtual-photon cross section based on the Generalized Parton Distributions [15] is in fair agreement with the magnitude of the data, at low values of $-t'$ and in the present Q^2 range, only if power corrections are included. In this kinematic region,

where π^+ production by longitudinal photons is expected to dominate, the data support the order of magnitude of the power corrections. A model calculation based on the Regge formalism for both the longitudinal and the transverse part of the cross section [37] provides a good description of the magnitude and the t' and the Q^2 dependences of the data.

We thank M. Guidal, J.M. Laget, and M. Vanderhaeghen for the theoretical calculations as well as M. Diehl for many interesting and useful discussions. We gratefully acknowledge the DESY management for its support, the staff at DESY and the collaborating institutions for their significant effort, and our national funding agencies and the EU RII3-CT-2004-506078 program for financial support.

[1] J.C. Collins, L. Frankfurt, and M. Strikman, Phys. Rev. D 56 (1997) 2982.
[2] D. Müller, D. Robaschik, B. Geyer, F.M. Dittes, and J. Horejsi, Fortschr. Phys. 42 (1994) 101.
[3] A.V. Radyushkin, Phys. Lett. B 380 (1996) 417.
[4] X. Ji, Phys. Rev. Lett. 78 (1997) 610.
[5] M. Burkardt, Phys. Rev. D 62 (2000) 071503; Erratum–ibid. D 66 (2002) 119903.
[6] M. Diehl, Eur. Phys. J. C 25 (2002) 223; Erratum-ibid. C31 (2003) 277.
[7] J.P. Ralston and B. Pire, Phys. Rev. D 66 (2002) 111501.
[8] A.V. Belitsky and D. Müller, Nucl. Phys. A 711 (2002) 118.
[9] M. Burkardt, Int. J. Mod. Phys. A 18 (2003) 173.
[10] K. Goeke, M.V. Polyakov, and M. Vanderhaeghen, Prog. Part. Nucl. Phys. 47 (2001) 401.
[11] M. Diehl, Phys. Rept. 388 (2003) 41.
[12] A.V. Belitsky and A.V. Radyushkin, Phys. Rept. 418 (2005) 1.
[13] W. R. Frazer, Phys. Rept. 115 (1959) 1763.
[14] J. D. Sullivan, Phys. Lett. B 33 (1970) 179.
[15] M. Vanderhaeghen, P.A.M Guichon, and M. Guidal, Phys. Rev. D 60 (1999) 094017.
[16] A.V. Belitsky and D. Müller, Phys. Lett. B 513 (2001) 349.
[17] M. Diehl and W. Kugler, *private communication*.
[18] P.D.B. Collins, Cambridge University Press, Cambridge (1977).
[19] M. Guidal, J.M. Laget, and M. Vanderhaeghen, Phys. Lett. B 400 (1997) 6.
[20] M. Vanderhaeghen, M. Guidal, and J.M. Laget, Phys. Rev. C 57 (1998) 1454.
[21] C.N. Brown *et al.*, Phys. Rev. D 8 (1973) 92.
[22] C.J. Bebek *et al.*, Phys. Rev. D 9 (1974) 1229; Phys. Rev. D 13 (1976) 25; Phys. Rev. D 17 (1978) 1693.
[23] P. Brauel *et al.*, Phys. Lett. B 65 (1976) 184; Phys. Lett. B 69 (1977) 253; Zeit. Phys. C 3 (1979) 101.
[24] J. Volmer *et al.*, Phys. Rev. Lett. 86 (2001) 1713.
[25] T. Horn *et al.*, Phys. Rev. Lett. 97 (2006) 192001.
[26] K. Ackerstaff *et al.*, Nucl. Instrum. Methods A417 (1998) 230.
[27] N. Akopov *et al.*, Nucl. Instrum. Methods A479 (2002) 511.
[28] T. Sjöstrand, L. Lonnblad, and S. Mrenna, Comput. Phys. Commun. 135 (2001) 238; P. Liebing, DESY-THESIS-2004-036.
[29] T. Sjöstrand, Comput. Phys. Commun. 82 (1994) 74.
[30] L.N. Hand, Phys. Rev. 129 (1963) 1834.
[31] R. Brun, R. Hagelberg, M. Hansroul, and J. Lassalle, CERN Report CERN-DD-78-2-REV (1978).
[32] I. Akushevich, H. Böttcher, and D. Ryckbosch, hep-ph/9906408 (1998).
[33] A. Ilyichev, *private communication*.
[34] L. Mankiewicz, G. Piller, and A. Radyushkin, Eur. Phys. J. C 10 (1999) 307.
[35] H. Abramowicz and A. Levy, hep-ph/9712415 (1997).
[36] L. Whitlow, S. Rock, A. Bodek, E. Riordan, and S. Dasu, Phys. Lett. B 250 (1990) 193.
[37] J.M. Laget, Phys. Rev. D 70 (2004) 054023.